17th World Conference on Earthquake Engineering, 17WCEE
Sendai, Japan - September 13th to 18th 2020

BI-DIRECTIONAL CONDITIONAL-SPECTRA-BASED RECORD SELECTION FOR HORIZONTAL AND VERTICAL GROUND MOTIONS

P. Bazzurro[(1)], M. Kohrangi[(2)], K, Bakalis[(3)], D. Vamvatsikos[(4)]

[(1)] *Professor, University School for Advanced Studies IUSS Pavia, paolo.bazzurro@iusspavia.it*
[(2)] *Risk Specialist, RED Risk Engineering + Development, mohsen.kohrangi@redrisk.it*
[(3)] *Research Associate, National Technical University of Athens, kbakalis@mail.ntua.gr*
[(4)] *Assistant Professor, National Technical University of Athens, divamva@mail.ntua.gr*

Abstract

Conditional Spectra (CS) based record selection is a state-of-the-art approach to select sets of records for performing nonlinear response time history analysis consistent with the seismic hazard at a specific site. So far this method has been developed and applied mainly to select horizontal components of the ground motion. There are many structural or nonstructural building components, however, and entire structures that are also sensitive to the vertical component of ground motion, e.g., due to concurrent vertical and horizontal deformability, uplifting and/or rocking. Thus, we aim here to further extend the CS approach to select a set of hazard consistent 3-component records. The proposed method is applied to the risk assessment of a liquid storage tank located at a site of major oil refineries in Elefsina, Greece. Tanks are prone to uplifting due to horizontal excitations, a behavior that can be exacerbated when the vertical component of the ground motion is considered. Therefore, a realistic seismic assessment of such structures cannot be carried out without simultaneously accounting for all three translational components of the ground motion. To this end in the case study we tested different record selection approaches with and without consideration of the vertical motions, as well as with and without vertical ground motions hazard consistency. Overall, there is a non-negligible dependence of the tank response to the effects of the vertical component, which should be included. Neglecting it typically result to an underestimation of about 20%. In addition, we recommend incorporating the hazard consistency of the vertical component in the record selection because it does have an impact on the tank response.

Keywords: Conditional spectra, record selection, vertical component, liquid storage tanks, seismic risk assessment

1. Introduction

Hazard-consistent record selection is a tool that prevents or limits bias in the assessment of seismic demand computed via nonlinear dynamic analysis. In recent years several studies have proven the need for hazard consistency of record selection proposing techniques such as CMS [1], CS [2] and GCIM [3]. These methods are designed to select records that are most representative of the earthquakes that control the seismicity of the site under investigation conditioned on the value of one or more intensity measures (*IM*s) of interest. At any single *IM* level, a set of records is selected (or artificially simulated) and scaled to match the conditioning *IM* value. The distributions of additional ground motion parameters, such as the spectral accelerations at other ordinates of the spectrum for CS, are conditioned to the *IM* value and to further characteristics (e.g. magnitude and distance) of earthquake scenarios relevant to the site hazard. While these methods are originally focused on record selection for dynamic analyses of 2D structural models, several recent studies have extended their application to horizontal bi-directional analyses of 3D models [4-6]. In particular, Kohrangi et al. [4] implemented multiple approaches for a bi-directional record selection, either by using a vector of *IM*s from both horizontal components in the CS, namely CS(vector), or by employing CS with a scalar *IM* while maintaining the consistency of both horizontal orthogonal components of the ground motion with the site hazard.

However, in all these studies the impact of the vertical component of the ground motion is neglected, while there are many examples of structural systems where this choice may not be warranted. Such examples include, but are not limited to, reinforced concrete precast structures [7], dams [8-10], components in nuclear

power plants [11], rocking systems [12], non-structural elements [13] (e.g. suspended ceilings), and building contents sensitive to rocking, sliding or overturning. As a result, when assessing the seismic performance of such structures using nonlinear dynamic analysis it would be advisable to account for the vertical ground motion component via sets of records that are compatible with the hazard at the site of interest. To assist in this endeavor, we extend the CS record selection methodology of Kohrangi et al. [4] for selecting sets of ground motion records that are compatible with both horizontal and vertical components of the site hazard, using scalar as well as vector valued intensity measures. The method is eventually implemented for a case study of an unanchored liquid storage tank located in a site of major oil refineries in Greece, offering a platform for discussing the effect of vertical acceleration and the associated CS-selection methods on global response parameters.

2. CS-based approaches including the vertical component

Including the vertical component in the standard CS approach of Lin et al. [14], where a scalar *IM* is employed as the conditioning variable, is a straightforward exercise of adding the vertical spectral acceleration ordinates in the joint lognormal model assumed therein. One only requires the correlation coefficients between the vertical spectral ordinates, as well as between the vertical and horizontal ones. Then, the algorithm of Jayaram et al. [2] may be employed to match the resulting conditional horizontal and vertical spectra targets to select records where all three components are compatible with the hazard.

On the other hand, the CS(vector) record selection approach [4] uses a vector of two or more intensity measures, e.g., $\boldsymbol{IM}^*=\{IM_1^*,\ IM_2^*\}$, as the conditioning *IM* instead of a single scalar. Note that bold characters, hereafter, represent vector variables. The focus of [4] was on *IM*s corresponding to the *horizontal* ground motion excitation, such as $\boldsymbol{IM}^*=\{Sa_x(T_{1x}),\ Sa_y(T_{1y})\}$ and $\boldsymbol{IM}^*=\{Sa_{g.m}(T_1),\ Sa_{g.m}(1.5T_1)\}$. The quantities $Sa_x(T_{1x})$ and $Sa_y(T_{1y})$ therein are defined as the spectral accelerations of the *x* and *y* components of the ground motion at the period of the first mode of vibration of the structure along the horizontal *x* and *y* axes, respectively. $Sa_{g.m}(T_1)$ and $Sa_{g.m}(1.5T_1)$ are the geometric means of the spectral accelerations at T_1 and $1.5\cdot T_1$ extracted from both horizontal components. As a candidate method to incorporate the vertical component, we extend the CS(vector) approach to select records by conditioning on $\boldsymbol{IM}^*=\{IM_h^*,\ IM_v^*\}$, where IM_h^* reflects the (geometric mean of the) horizontal intensity of the ground motion and IM_v^* corresponds to its vertical intensity.

In general, of interest is the generation of a target spectrum distribution conditioned on the joint occurrence of $\ln IM_h^*=x_h$ and $\ln IM_v^*=x_v$ for given magnitude (M), site-to-rupture distance (R) and other applicable site characteristics. Let this spectrum be represented by the vector $\boldsymbol{SA}=\{Sa(T_{a1}),\ Sa(T_{a2}),\ldots,\ Sa(T_{an})\}$, where T_{a1} to T_{an} are the n periods of interest. As customarily done, it is assumed that $\boldsymbol{SA}$ follows a joint lognormal distribution. Then, its logarithmic mean, $\boldsymbol{\mu}$, can be shown to be [4]:

$$\boldsymbol{\mu}=\begin{bmatrix}\mu_{\ln Sa(T_{a1})|\ln IM_h^*=x_h,\ln IM_v^*=x_v,m,r}\\ \mu_{\ln Sa(T_{a2})|\ln IM_h^*=x_h,\ln IM_v^*=x_v,m,r}\\ \vdots\\ \mu_{\ln Sa(T_{an})|\ln IM_h^*=x_h,\ln IM_v^*=x_v,m,r}\end{bmatrix}=\begin{bmatrix}\mu_{\ln Sa(T_{a1})|m,r}+\mathbf{H}_{vh}^{(T_{a1})}\cdot\mathbf{H}_{hh}^{-1}\cdot\begin{bmatrix}x_h-\mu_{\ln IM_h^*|m,r}\\ x_v-\mu_{\ln IM_v^*|m,r}\end{bmatrix}\\ \mu_{\ln Sa(T_{a2})|m,r}+\mathbf{H}_{vh}^{(T_{a2})}\cdot\mathbf{H}_{hh}^{-1}\cdot\begin{bmatrix}x_h-\mu_{\ln IM_h^*|m,r}\\ x_v-\mu_{\ln IM_v^*|m,r}\end{bmatrix}\\ \vdots\\ \mu_{\ln Sa(T_{an})|m,r}+\mathbf{H}_{vh}^{(T_{an})}\cdot\mathbf{H}_{hh}^{-1}\cdot\begin{bmatrix}x_h-\mu_{\ln IM_h^*|m,r}\\ x_v-\mu_{\ln IM_v^*|m,r}\end{bmatrix}\end{bmatrix},\qquad(1)$$

where $\mu_{\ln Sa(T_{ai})|\ln IM_h^*=x_h,\ln IM_v^*=x_v,m,r}$ is the logarithmic mean of the spectral acceleration at period T_{ai}, where $i=1,\ldots,n$, conditioned on the joint occurrence of the vector $\left\{\ln IM_h^*=x_h,\ln IM_v^*=x_v\right\}$, for an assumed scenario

with magnitude, $M = m$, and site-to-rupture distance, $R = r$. The quantity $\mu_{\ln Sa(T_{ai})|m,r}$ is the logarithmic mean of the spectral acceleration at period T_{ai} obtained from the ground motion prediction equation (GMPE) of choice for horizontal and vertical components estimated for the m and r scenario parameter values. The $\mathbf{H}_{ij}$ are sub-matrices of matrix $\mathbf{H}$:

$$\mathbf{H}^{(T_{ai})} = \begin{bmatrix} \mathbf{H}_{hh} & \mathbf{H}_{hv}^{(T_{ai})} \\ \mathbf{H}_{vh}^{(T_{ai})} & \mathbf{H}_{vv}^{(T_{ai})} \end{bmatrix}. \tag{2}$$

Note that $\mathbf{H}_{hh}$ in Equation (2) depends only on the vector ***IM**** but it is independent of T_{ai}, whereas $\mathbf{H}_{vh}$, $\mathbf{H}_{hv}$ and $\mathbf{H}_{vv}$ are functions of the spectral accelerations at period T_{ai}. The elements of matrix $\mathbf{H}$ are defined as follows:

$$\mathbf{H}_{hh} = \begin{bmatrix} \sigma^2_{\ln IM_h^*|m,r} & \rho_{\ln IM_h^*,\ln IM_v^*}\sigma_{\ln IM_h^*|m,r}\sigma_{\ln IM_v^*|m,r} \\ \rho_{\ln IM_h^*,\ln IM_v^*}\sigma_{\ln IM_h^*|m,r}\sigma_{\ln IM_v^*|m,r} & \sigma^2_{\ln IM_v^*|m,r} \end{bmatrix}, \tag{3}$$

$$\mathbf{H}_{vh}^{(T_{ai})} = \left(\mathbf{H}_{hv}^{(T_{ai})}\right)' = \left[\rho_{\ln Sa(T_{ai}),\ln IM_h^*}\sigma_{\ln Sa(T_{ai})|m,r}\sigma_{\ln IM_h^*|m,r} \quad \rho_{\ln Sa(T_{ai}),\ln IM_v^*}\sigma_{\ln Sa(T_{ai})|m,r}\sigma_{\ln IM_v^*|m,r}\right]. \tag{4}$$

$$\mathbf{H}_{vv}^{(T_{ai})} = \sigma^2_{\ln Sa(T_{ai})|m,r}, \tag{5}$$

The quantities $\sigma^2_{\ln IM_v^*|m,r}$ and $\sigma^2_{\ln IM_v^*|m,r}$ are the variances of $\ln IM_h^*$ and $\ln IM_v^*$, respectively, and $\rho_{\ln IM_h^*,\ln IM_v^*}$ is their correlation coefficient. The quantity $\rho_{\ln Sa(T_{ai}),\ln IM^*}$ is the correlation coefficient between $\ln Sa(T_{ai})$ and $\ln IM^*$. Now, let $\mathbf{\Sigma}_0$ denote the (unconditional) covariance matrix of the vector ***SA***:

$$\mathbf{\Sigma_0} = \begin{bmatrix} \sigma^2_{\ln Sa(T_{a1})} & \cdots & \rho_{\ln Sa(T_{a1}),\ln Sa(T_{an})}\cdot\sigma_{\ln Sa(T_{a1})}\cdot\sigma_{\ln Sa(T_{an})} \\ \vdots & \ddots & \vdots \\ \rho_{\ln Sa(T_{an}),\ln Sa(T_{a1})}\cdot\sigma_{\ln Sa(T_{an})}\cdot\sigma_{\ln Sa(T_{a1})} & \cdots & \sigma^2_{\ln Sa(T_{an})} \end{bmatrix}, \tag{6}$$

Let $\mathbf{\Sigma}_1$ denote the covariance matrix of ***SA*** and ***IM**** $=\{IM_h^*, IM_v^*\}$, which can be shown to be [4]:

$$\mathbf{\Sigma_1} = \begin{bmatrix} \mathbf{H}_{vh}^{(T_{a1})}\cdot\mathbf{H}_{hh}^{-1}\cdot\mathbf{H}_{hv}^{(T_{a1})} & \mathbf{H}_{vh}^{(T_{a1})}\cdot\mathbf{H}_{hh}^{-1}\cdot\mathbf{H}_{hv}^{(T_{a2})} & \cdots & \mathbf{H}_{vh}^{(T_{a1})}\cdot\mathbf{H}_{hh}^{-1}\cdot\mathbf{H}_{hv}^{(T_{an})} \\ \vdots & & \ddots & \vdots \\ \mathbf{H}_{vh}^{(T_{an})}\cdot\mathbf{H}_{hh}^{-1}\cdot\mathbf{H}_{hv}^{(T_{a1})} & \mathbf{H}_{vh}^{(T_{an})}\cdot\mathbf{H}_{hh}^{-1}\cdot\mathbf{H}_{hv}^{(T_{a2})} & \cdots & \mathbf{H}_{vh}^{(T_{an})}\cdot\mathbf{H}_{hh}^{-1}\cdot\mathbf{H}_{hv}^{(T_{an})} \end{bmatrix}. \tag{7}$$

Following Johnson and Wichern [15] the covariance matrix of ***SA*** conditioned on ***IM**** is:

$$\mathbf{\Sigma} = \mathbf{\Sigma}_0 - \mathbf{\Sigma_1} \tag{8}$$

Equations (1) and (8) essentially provide us with all the needed information to define the joint lognormal distribution of ***SA***.

3. Case study structure and modeling approach

The record selection methodology above is applied to the assessment of a tank shown in Fig. 1(a). This structure is an excellent case study to investigate the suitability of the aforementioned CS selection techniques, due to the uplift (i.e., vertical) motion that it may exhibit under severe ground motion excitation [16], even if only the horizontal component is applied. The radius (R_t) of the case study tank is 13.9m and its height (H_t) is 16.5m. The tank is assumed to be filled with water (i.e. density ρ=1,000kg/m^3) at a maximum operating fluid level (h_f) of 15.7m. The design of the wall comprises 9 equally spaced courses, the thickness of which ranges from 17.7mm (bottom course) to 6.4mm (top course). In addition, the base of the tank shell

consists of an inner base plate of thickness t_b=6.4mm and an outside annular plate of t_a=8.0mm. All steel plates are made of grade S235 steel.

The 3D "joystick" surrogate model [Fig. 1(b)] developed by Bakalis et al. [17] is adopted to conduct nonlinear response history analysis. This model consists of a single mass that activates the impulsive fluid component (m_i) in both horizontal directions [18] and the entire fluid mass (m_l) in the vertical. This mass is attached to an elastic beam-column element, whose properties are estimated such that the fundamental period of the model is fully aligned with the theoretical solution for the impulsive period [19]. The elastic element is connected to N rigid beam-spokes that rest on multilinear elastic edge-springs. Those springs are assigned uplift (w) as well as compression resistance properties of a beam "strip" model that extends radially on the base plate of the tank. This model has an effective width $b_w=2\pi R_t/N$, utilises rotational and axial springs to represent the plate-wall interaction, has a concentrated force and moment to take into account the effect of hydrostatic loads, and is supported by an elastic tensionless Winkler soil/foundation. Essentially, the "Joystick" model is a two-stage model that requires the execution of the base-plate strip model "pre-analysis" step to determine the properties of the edge-springs (e.g., vertical force versus uplift, separation length, etc.) of the "Joystick" model.

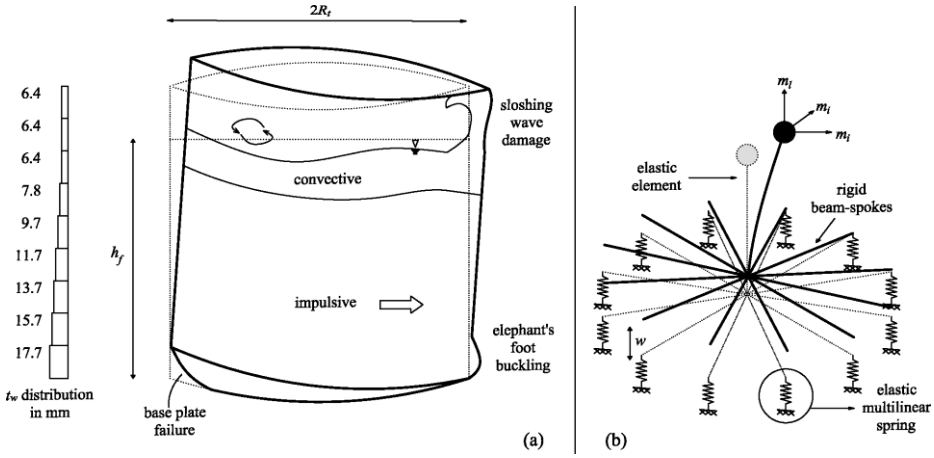

Fig. 1 – (a) Impulsive versus convective fluid component, and properties of the case study liquid storage tank; (b) the "joystick" surrogate model [17] and its deflected shape.

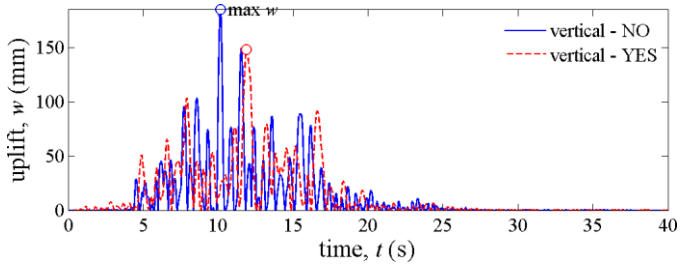

Fig. 2 – Tank uplift response history, featuring the effect of vertical component for a single ground motion record.

4. Hazard analysis and ground motion database

A site of major oil refineries in Elefsina, Greece with coordinates of (23.507°E, 38.04°N) is adopted to perform all probabilistic seismic hazard analysis (PSHA) computations. OpenQuake [21], the open-source software for seismic hazard and risk assessment, is used to perform the seismic hazard and disaggregation computations. PSHA and Vector PSHA (VPSHA) computations, the latter based on the *indirect* approach [25], are based on the SHARE Project [22] area source model. The ground motion prediction equation (GMPE) of Abrahamson et al. [23] and Gülerce et al. [24] were used for the horizontal and vertical spectral

accelerations, respectively. We carried out seismic response analysis of the selected liquid storage tank using four hazard-consistent variants of record selection, all based on the CS method. Table 1 describes both the conditioning *IM** and the assumptions considered in the record selection for each variant. In all cases, the conditioning scalar *IM** adopted in the horizontal plane is the geometric mean of spectral acceleration from both horizontal components of the ground motion, $Sa_h(T_i)$ at a period of T_i = 0.3s. This may not precisely match the impulsive period, yet it is close enough for all practical purposes of record selection. In the vertical direction, Sa_v(0.3s) was chosen mainly for reasons of simplicity. It may be different from the vertical period of 0.1s, yet at such short periods there is little difference between the two. Actually, given the overall uncertainty in periods and the jagged nature of the spectra in the short period range, exploring IMs such as *AvgSA* [26] would perhaps be more appropriate.

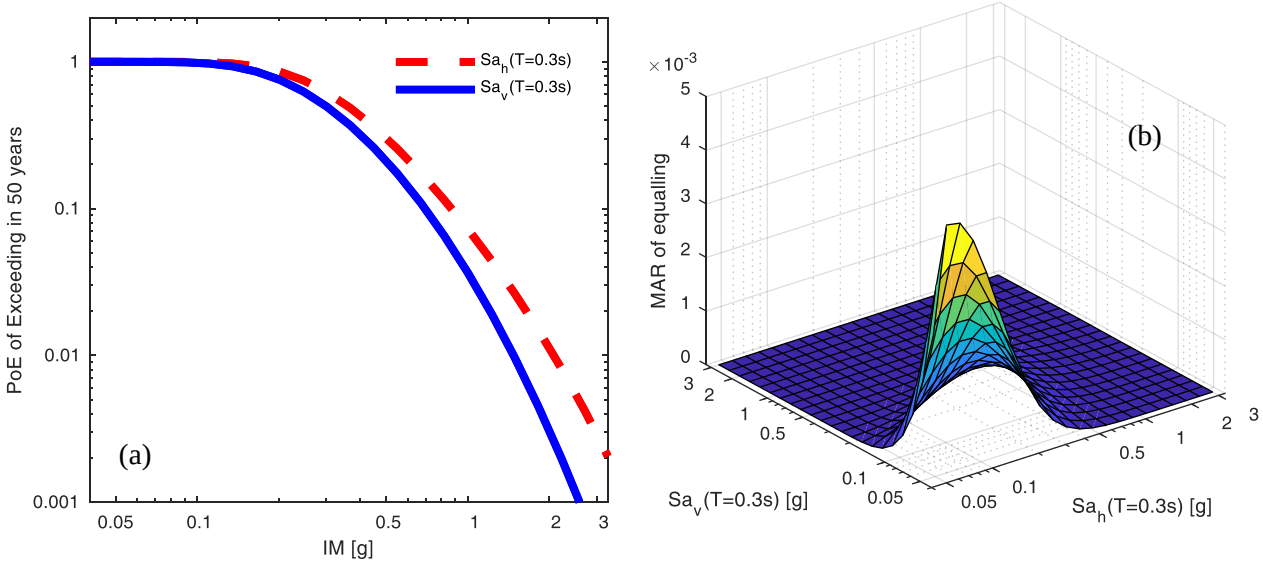

Fig. 3 – PSHA results: a) Hazard curves using scalar IMs; (b) VPSHA mean annual rate of equaling.

The target spectra for each conditioning *IM** were based on the mean M-R scenarios obtained from the disaggregation results of PSHA and VPSHA for the selected site. This approach is referred to as the *approximate* method versus the *exact* method in which all the causal events in the disaggregation analysis are considered in generating the target spectrum [14]. The correlation coefficients for the horizontal-horizontal components SAs are defined based on Baker and Jayaram [27] while the correlations between vertical-vertical and vertical-horizontal components SAs are adopted from Kohrangi et al. [28]. For the first record set (Case 1 in Table 1), we neglect the impact of the vertical component of the ground motion and, therefore, we carried out the common CS based record selection for the horizontal components of the ground motion (specifically their geometric mean). Case 2 and Case 3 in Table 1 extend Case 1 to include the vertical component. In Case 2, we selected and scaled the records to match the target spectrum only for the (geomean) horizontal component of the ground motion. The vertical component in this case, scaled by the same factor, is utilized regardless of its consistency with the site hazard. We label this approach as "R" (Table 1) because one of the components is chosen *regardless* of its hazard consistency. In the arguably superior Case 3 approach, we consider both horizontal and vertical components of the ground motion as the target spectrum, taking into account the correlation of the spectral accelerations. This approach is labeled as "C" (Table 1) because of its *compatibility* (or consistency) with the hazard for both horizontal and vertical components of the ground motion. For the three aforementioned record selection cases, we selected suites of 77 records (each with three components for Cases 2 and 3 and two components for Case 1) to match the target spectrum corresponding to seven *IM* levels with central bin values of 0.36, 0.86, 1.15, 1.62, 2.04, 2.39 and 3.21g at Sa_h(0.3s). The selected *IMs*' return periods of exceedance for the site of interest range from 10 to 5,000 years. Note that here we used the CS record selection algorithm of Jayaram et al. [2], modified for Case 3, i.e. CS[$S_{ah}(T_i)$]-C, to consider the spectral ordinates at both horizontal and vertical components as well as the correlation structures of spectral ordinates for both.

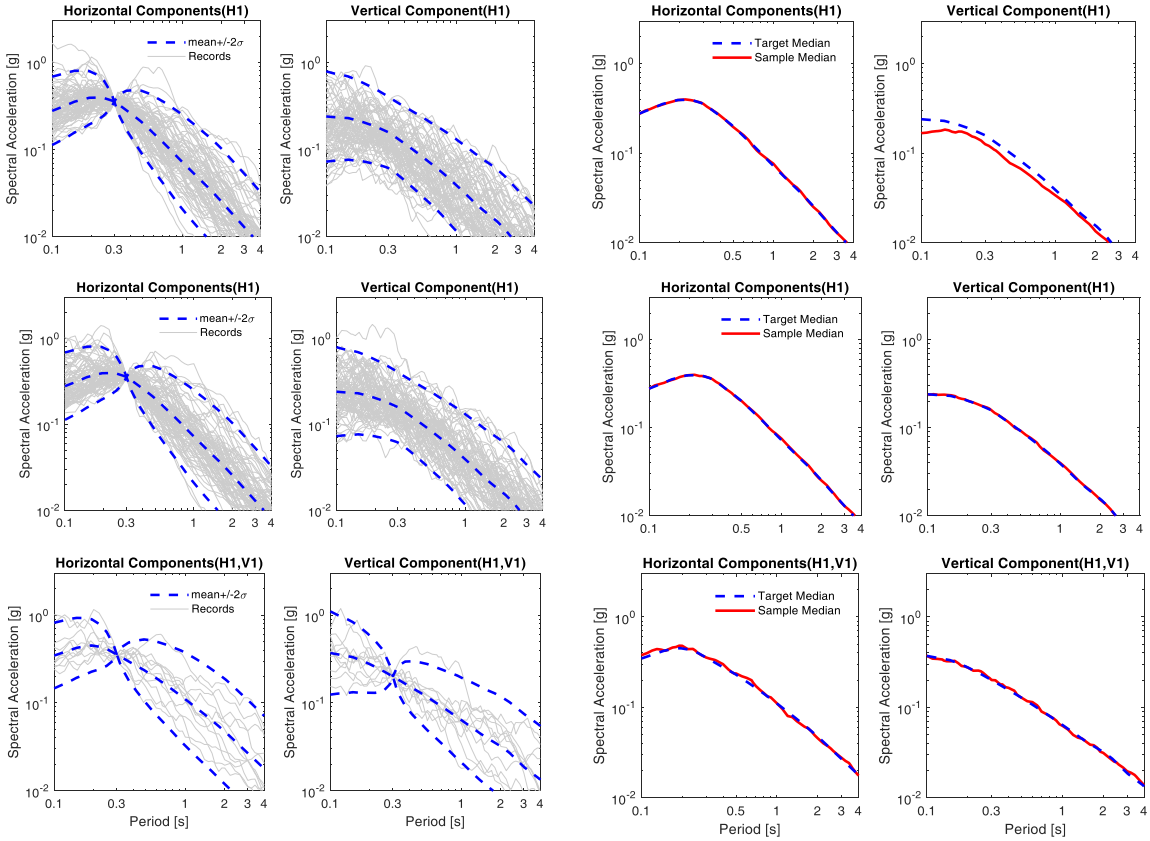

Fig. 4 – Illustration of the CS record sets used for the analysis. Rows from left: **First:** CS-R for a scenario with Sa_h(0.3s)=0.4g; **Second:** CS-C for a scenario with Sa_h(0.3s)=0.4g; **Third:** CS{$Sah(T_i)$, $Sa_v(T_i)$} for a scenario with Sa_h(0.3s)=0.4g, Sa_v(0.3s)=0.2g. Note: the left two columns shows the target spectra in blue lines and the spectra of the selected records in grey lines; the two columns in right show the target spectra in blue and the median spectra of the selected records in red.

Table 1 – Conditional spectra-based record selection variants and the adopted assumptions

Case No.	Notation	Conditioning *IM* for CS selection	Record selection description
1	CS_{xy}	Scalar: Geometric mean of spectral acceleration of two horizontal components at T_i, $Sa_h(T_i)$.	Records are selected and scaled to match the target spectrum of the (geomean) horizontal spectral acceleration, *no vertical* component is applied.
2	CS-R_{xyz}	As in Case 1	Records are selected and scaled to match the target spectrum of the (geomean) horizontal spectral acceleration. The (scaled) vertical component is inherited and used *regardless* of its spectral shape hazard consistency.
3	CS-C_{xyz}	As in Case 1	Records are selected and scaled to match the target spectrum of the (geomean) horizontal and vertical components considering the correlation of spectral accelerations. The spectral shapes at both horizontal and vertical components are, therefore, *compatible* with the hazard.
4	CS-V_{xyz}	Vector: Spectral accelerations of both horizontal and vertical components of the ground motion at T_i, ***IM****=$\{Sa_h(T_i), Sa_v(T_i)\}$.	Records are selected and scaled to match the target spectra of both horizontal and vertical components considering the correlation of the spectral accelerations. The spectral shape at both horizontal and vertical components are, therefore, *compatible* with the hazard.

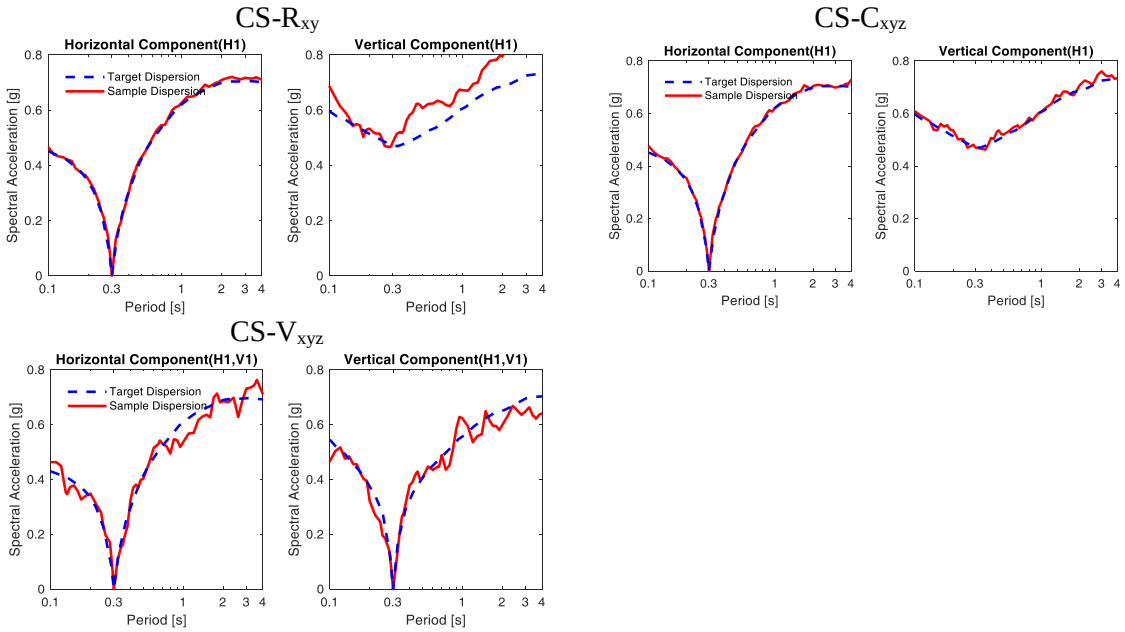

Fig. 5 – Illustration of the CS record sets used for the analysis. The target spectra are shown in blue and the conditional standard deviation of the spectra for the selected records in red.

Furthermore, we defined a vector ***IM**** (Case 4 in Table 1), consisting of two scalar *IM*s computed from the horizontal and vertical ground motion components, namely ***IM**** $=\{Sa_h(T_i), Sa_v(T_i)\}$. We discretized the 2D *IM** domain of horizontal and vertical ground motions into 7×7=49 cells centered at acceleration values equal to 0.36, 0.86, 1.15, 1.62, 2.04, 2.39 and 3.21g for the horizontal component, as before, and 0.20, 0.49, 0.65, 0.91, 1.14, 1.32 and 1.75g for the vertical component. In this case, for each cell we selected 11 records including all three components (for a total of 539) that best match the target spectra. For comparison purposes, one may think of aggregating a single row (or column) of seven cells from a vector ***IM**** to make a stripe conditioned on a single value of the (non-aggregated) scalar *IM*. Thus 7×11 = 77 records have been employed per "stripe" of (a single element of) vector *IM*s vis-à-vis the 77 records of scalar *IM* cases.

5. Results

Nonlinear dynamic analyses of the case study liquid storage tank were performed for each intensity level and associated records. For brevity, we only show the results of the maximum tank uplift as the engineering demand parameter (EDP). Fig. 6a compares the maximum tank uplift response stripes obtained from the four record selection approaches delineated earlier. The maximum tank uplift is limited to 100 cm assuming that values more than this threshold cause collapse of the structure (i.e., uncontrolled content release). In order to show the impact of the vertical ground motion on the maximum tank uplift, the EDP response for Case 2 is divided by the EDP value of corresponding analysis in Case 1. Fig. 6b shows the boxplot of this ratio suggesting that, on average, there is an increase in the response when the vertical component of the ground motion is applied. Fig. 7a compares the absolute uplift hazard curve (mean annual rate of exceeding, λ) obtained from the four different approaches while Fig. 7b shows the ratio of the λ values of Case *i*/Case 1. Overall, the results of Case 4 (vector IM) appear lower but those results are subject to some noise, due to how one chooses to represent the more elaborate fragility surface for a vector IM and integrate it with the equally elaborate VPSHA hazard surface (Fig. 3b). Hence, no concrete conclusion can be thus derived for the vector approach until more application options are explored. For the scalar IMs variants, it is obvious that appropriately considering the vertical component (Case 3) does make a difference. For this structure it produces larger uplift values than those obtained with only horizontal components. Also it is advisable to

include the vertical component in a hazard-consistent way. Still, obviously this is only a single case study and many more will be required before such conclusions can be generalized.

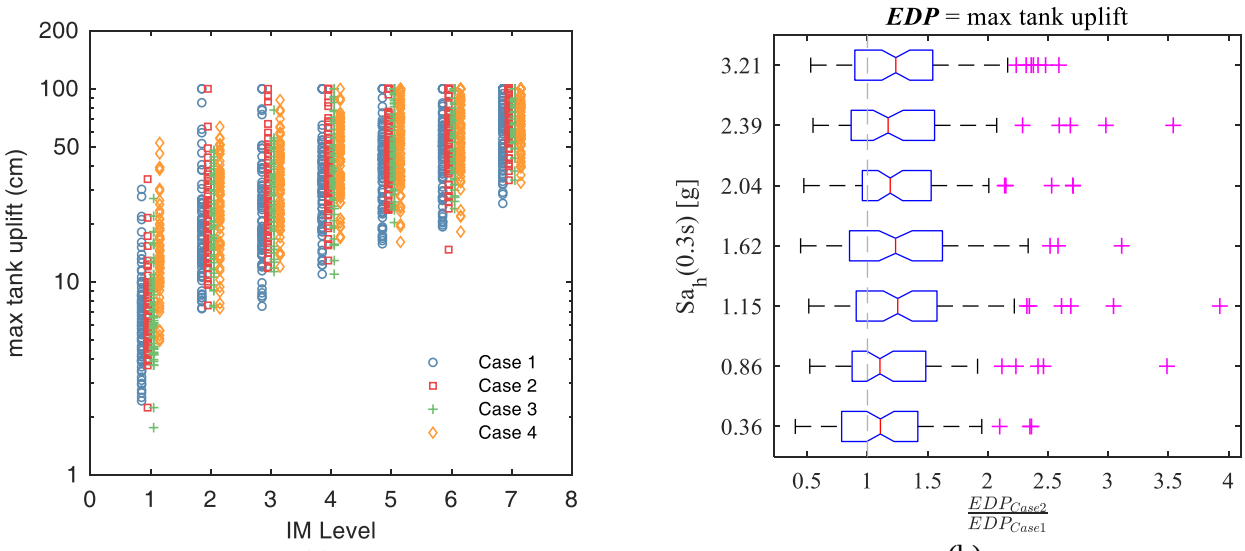

(a) (b)

Fig. 6 – Results of MSA. (a) Comparing the maximum uplift of the tank based different record selection approaches; (b) response ratio obtained from Case 2 over Case 1.

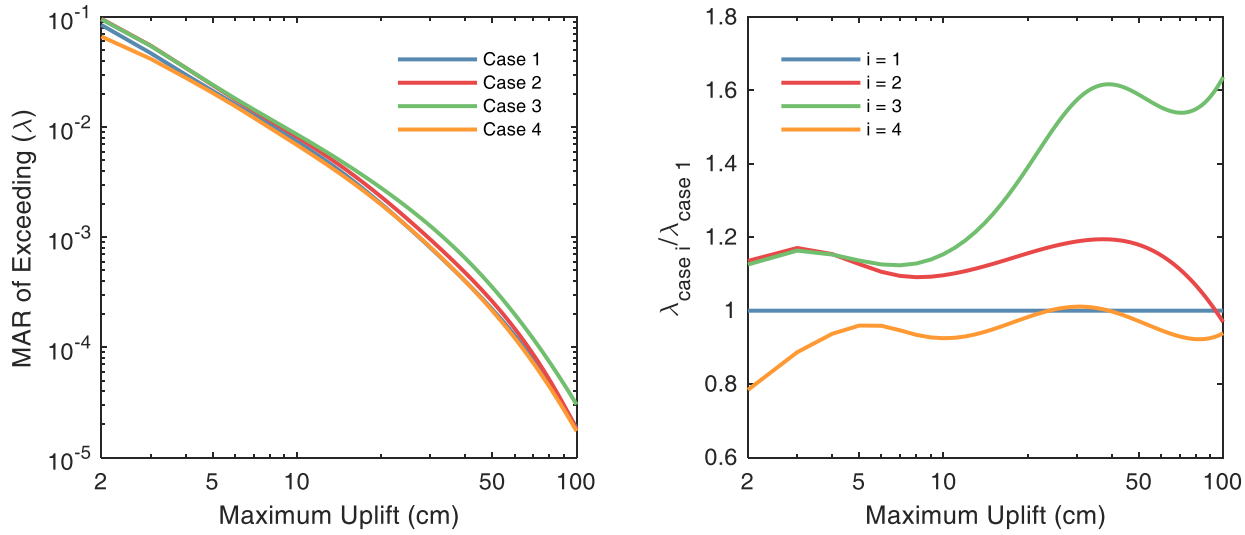

(a) (b)

Fig. 7 – (a) Comparison between the response hazard curves (mean annual rate of exceeding, λ) in terms of maximum uplift of the tank using different record selection approaches of this study; (b) relative $\lambda_{case\ i}/\lambda_{case\ 1}$.

6. Conclusions

Different conditional-spectrum-based record selection approaches with four different assumptions in terms of accounting (or not) for the vertical component of the ground motion are addressed herein. We used both scalar and vector intensity measures as conditioning IMs taking different routes to selection. In one case no vertical component is considered, while in other three approaches the vertical component is accounted for to a different degree of sophistication. We tested these four approaches on the risk assessment of a liquid storage tank located at a site in Elefsina, Greece. Multiple stripe analysis is performed and the response of

the tank in terms of maximum uplift is monitored. The results show that ignoring the impact of the vertical component of the ground motion results in an underestimation of the maximum uplift demand. We also observe that using an approach that accounts for the hazard consistency of the ground motion can improve the risk estimates, at least in terms of the uplift of this unanchored tank. The record-selection methodologies described here can be applied to a wide range of structures that sensitive to vertical motion to achieve hazard consistency in the vertical direction. Still, whether the effect of vertical ground motion components is important enough to be considered depends on the structure and on the objective of the risk assessment.

7. References

[1] Baker JW (2011): Conditional Mean Spectrum: Tool for ground motion selection. *Journal of Structural Engineering*, **137** (3), 322–331.
[2] Jayaram N, Lin T, Baker J (2011): A Computationally Efficient Ground-Motion Selection Algorithm for Matching a Target Response Spectrum Mean and Variance. *Earthquake Spectra* 2011. **27** (3), 797–815.
[3] Bradley BA (2010): A generalized conditional intensity measure approach and holistic ground-motion selection. *Earthquake Engineering & Structural Dynamics*. **39** (12), 1321–1342.
[4] Kohrangi M, Bazzurro P, Vamvatsikos D (2019): Conditional spectrum bidirectional record selection for risk assessment of 3D structures using scalar and vector IMs. *Earthquake Engineering & Structural Dynamics*, **48** (9), 1066–1082.
[5] Beyer K, Bommer JJ (2007): Selection and Scaling of Real Accelerograms for Bi-Directional Loading: A Review of Current Practice and Code Provisions. *Journal of Earthquake Engineering*, **11**(sup1), 13–45.
[6] Niveas C, Timothy S (2018): A multidirectional conditional spectrum. *Earthquake Engineering & Structural Dynamics*, **47** (4), 945–965.
[7] Bovo M, Savoia M (2019): Evaluation of force fluctuations induced by vertical seismic component on reinforced concrete precast structures. *Engineering Structures*, **178**, 70–87.
[8] Chopra AK (1966): The importance of the vertical component of earthquake motions. *Bulletin of the Seismological Society of America*, **56** (5), 1163–1175.
[9] Chakrabarti P, Chopra AK (1972): Hydrodynamic pressures and response of gravity dams to vertical earthquake component. *Earthquake Engineering and Structural Dynamics*, **1** (14), 325–335.
[10] Christopoulos C, Léger P, Filiatrault A (2003): Sliding response of gravity dams including vertical seismic accelerations. *Earthquake Engineering and Engineering Vibration*, **2** (2), 189–200.
[11] Kitamura S, Okamura S, Takahashi K (2005): Experimental Study on Vertical Component Seismic Isolation System With Coned Disk Spring, in Proceedings of the ASME 2005 Pressure Vessels and Piping Conference. Volume 8: Seismic Engineering: Denver, Colorado, USA, 175–182.
[12] Vrettos C (1999): Vertical and rocking impedances for rigid rectangular foundations on soils with bounded non-homogeneity. *Earthquake Engineering & Structural Dynamics*, **28** (12), 1525–1540.
[13] Moschen L, Medina RA, Adam C (2016): Vertical acceleration demands on column lines of steel moment-resisting frames. *Earthquake Engineering & Structural Dynamics*, **45** (12), 2039–2060.
[14] Lin T, Harmsen SC, Baker JW, Luco N (2013): Conditional spectrum computation incorporating multiple causal earthquakes and ground motion prediction models. *Bulletin of Seismological Society of America*, **103** (2A), 1103–1116.
[15] Johnson RA, Wichern SW (2007): *Applied Multivariate Statistical Analysis*. Prentice Hall, Upper Saddle River, NJ.
[16] Haroun MA, Tayel MA (1985): Response of tanks to vertical seismic excitations. *Earthquake Engineering & Structural Dynamics*, **13** (5), 583–595.
[17] Bakalis K, Fragiadakis M, Vamvatsikos D. (2017). Surrogate modeling for the seismic performance assessment of liquid storage tanks. *Journal of Structural Engineering*, **143** (4), 04016199.
[18] Malhotra PK, Veletsos AS (1994): Uplifting response of unanchored liquid storage tanks. *Journal of Structural Engineering*, **120** (12), 3525–3547.
[19] Eurocode 8 (2004): *Design of structures for earthquake Resistance — Part 1: general rules, seismic actions and rules for buildings*, Comité Européen de Normalisation: Brussels, Belgium.
[20] Chiou B, et al. (2008): NGA Project Strong-Motion Database. *Earthquake Spectra*, **24** (1), 23–44.
[21] Monelli D, Pagani M, Weatherill G, Silva V, Crowley H (2012): The hazard component of OpenQuake: The calculation engine of the Global Earthquake Model. *15th World Conference on Earthquake Engineering*, Lisbon, Portugal.
[22] Giardini D, et al. (2013): Seismic Hazard Harmonization in Europe (SHARE). Online data resource, Swiss Seismological Service, ETH Zurich, Zurich, Switzerland, [Available at: http://www.efehr.org:8080/jetspeed/].

[23] Abrahamson NA, Silva WJ, Kamai R. (2014). Summary of the ASK14 ground motion relation for active crustal regions. *Earthquake Spectra*, **30** (3), 1025–1055.
[24] Gülerce Z, et al. (2017): Ground motion prediction equations for the vertical ground motion component based on the NGA-W2 Database. *Earthquake Spectra*, **33** (2), 499–528.
[25] Kohrangi M, Bazzurro P, Vamvatsikos D (2016): Vector and scalar IMs in structural response estimation, Part I: Hazard analysis. *Earthquake Spectra*, **32** (3), 1507–1524.
[26] Bakalis K, Kohrangi M, Vamvatsikos D (2018): Seismic intensity measures for above-ground liquid storage tanks. *Earthquake Engineering & Structural Dynamics*, **47** (9), 1844–1863.
[27] Baker JW, Jayaram N (2008): Correlation of spectral acceleration values from NGA ground motion models. *Earthquake Spectra*, **24**, 299–317.
[28] Kohrangi M, et al. (2019): Correlation of spectral acceleration values of vertical and horizontal ground motion pairs. *Earthquake Spectra* (Under review).

